A candidate mechanism for exciting sound during bubble coalescence

Helen Czerski
Institute of Sound and Vibration Research, University of Southampton, Highfield, Southampton, Hampshire SO17 1BJ, UK
H.Czerski.97@cantab.net

Abstract: Coalescing bubbles are known to produce a pulse of sound at the moment of coalescence, but the mechanism driving the sound production is uncertain. A candidate mechanism for the acoustic forcing is the rapid increase in the bubble volume, as the neck of air joining the two parent bubbles expands. A simple model is presented here for the volume forcing caused by the coalescence dynamics, and its predictions are tested against the available data. The model predicts the right order of magnitude for the acoustic amplitude, and the predicted amplitudes also scale correctly with the radius of the smaller parent bubble.

PACS numbers: 43.30.Nb [AL]
Date Received: November 22, 2010 **Date Accepted:** January 10, 2011

1. Introduction

The pulses of sound produced by newly formed bubbles are of interest to a wide range of scientific fields because they provide information about changes occurring in a bubble population. Past research has tended to focus on the sounds produced as bubbles fragment, but it has long been known[1,2] that an acoustic signal is also emitted at the moment that two bubbles coalesce. This signal has the form of a decaying sinusoid at the natural frequency of the new larger bubble. The pressure amplitude depends on the mechanism driving the new bubble into volume oscillations, and to date no study has conclusively identified the mechanism exciting the sound pulse. Manasseh *et al.*[3] have investigated the pressure jump due to the equalization of pressures, and found that this mechanism produced the right scaling in amplitude with bubble radius. However, the magnitude of the amplitude was under-predicted by an order of magnitude.

Recent research[4] has shown that the sound emitted when a new bubble is formed at a nozzle is consistent with the volume forcing produced by the rapid change in bubble shape just after pinch-off. The collapse of the conical neck of air that had connected the new bubble to the parent gas supply is fast because the radius of curvature of the new surface is very small. Consequently, the bubble volume changes on a timescale far shorter than the natural frequency of the bubble and this drives volume oscillations and acoustic emission. This paper was motivated by the observation that a similar (but inverted) situation occurs when two bubbles touch and start to coalesce. The two bubbles (assumed spherical here) first touch at a point, and an approximately cylindrical neck of air joining the two bubbles is formed. The boundary surface between the gas and liquid then has a very small radius of curvature and there is no balancing force to maintain this situation. The liquid accelerates outward, rapidly increasing the total volume of the new bubble. The aim of this paper is to present simple calculations to examine whether this rapid volume change could explain the observed acoustic amplitudes when bubbles coalesce. A dynamical model of the volume change on coalescence will be described here, following the principles used in Deane and Czerski.[4] The consequent dynamical and acoustical predictions will be tested against the data published by Thoroddsen *et al.*[5] and Manasseh *et al.*[3]

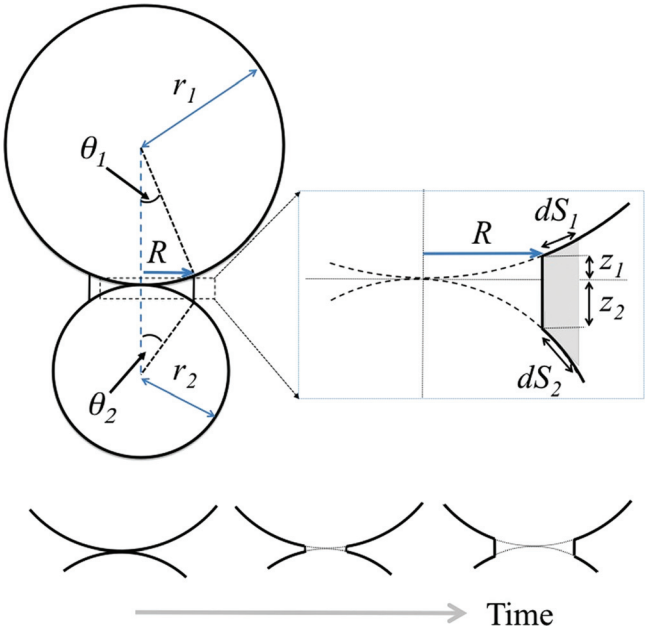

Fig. 1. (Color online) Diagram showing the parameters used for the model described here. The two bubbles (with radii r_1 and r_2) are considered axisymmetric about the line joining their centers. R is the radius of the neck of air joining them (which is assumed cylindrical). The inset shows a close-up of the region where the two bubbles touch, and the shaded area shows the cross-section of the liquid annulus under consideration in the model when the neck has reached radius R. The schematic diagrams along the bottom of the panel show how the neck is assumed to change in time, where the solid lines represent the actual bubble walls at any time and the dotted lines show the initial position of the bubble walls.

2. Dynamical model

The model is based on energy balance arguments. In order to carry out a simple first-order calculation, we assume that thermal and viscous losses are negligible on the short timescales considered here. Figure 1 defines the geometry and the parameters used in the calculation. The situation is axisymmetric about a line joining the bubble centers, and we make no assumptions about their relative sizes.

At time zero, the bubbles touch at a single point, and the neck of air joining them is assumed to be infinitesimally thin. This is the moment of formation of a new bigger bubble. We will assume here that the neck is cylindrical, even though Thoroddsen *et al.*[5] showed that arcs of circles can be fitted to the shape of the bubble wall. The reason for this simplification is that it permits an analytic solution for the neck radius with time, while still including the fundamental physics of the problem. Consider an annulus of liquid just outside the neck, when the neck has a radius of R. We assume that the surface area that will be lost as this annulus moves outwards from R to $R+dR$ in time dt provides the kinetic energy for that annulus to move outwards at a speed dR/dt:

$$2\pi R(dS_1 + dS_2 - dz_1 - dz_2)\sigma = \frac{1}{2}(2\pi R(z_1 + z_2)dR)\rho\left(\frac{dR}{dt}\right)^2, \quad (1)$$

where dS_1 and dS_2 are the widths of the slanted areas lost from bubbles 1 and 2, and $z_1 + z_2$ is the height of the new surface area formed (vertical in Fig. 1). σ is the surface tension and ρ is the density of the liquid.

We can rearrange Eq. (1) in terms of r_1, r_2, θ_1, and θ_2 (all defined in Fig. 1) to get an expression for the outward velocity,

$$\left(\frac{dR}{dt}\right)^2 = \frac{2\sigma}{\rho}\left(\frac{\frac{1}{\cos\theta_1}\left(1-\frac{R}{r_1}\right)+\frac{1}{\cos\theta_2}\left(1-\frac{R}{r_2}\right)}{r_1(1-\cos\theta_1)+r_2(1-\cos\theta_2)}\right). \tag{2}$$

Using $R/r_1 = \sin\theta_1$, $R/r_2 = \sin\theta_2$ and the approximations $\cos\theta_1 \approx 1 - R/2r_1^2$, and $\cos\theta_2 \approx 1 - R^2/2r_2^2$, we can eliminate θ_1 and θ_2,

$$\left(\frac{dR}{dt}\right)^2 = \frac{4\sigma}{\rho R^2}\left(\frac{2r_1r_2}{r_1+r_2} - R + \frac{R^2}{2}\frac{r_2^2+r_1^2}{r_2^2r_1+r_1^2r_2}\right). \tag{3}$$

Equation (3) is valid to second order and is presented for completeness. The most important forcing will occur at small values of R, so to make the expression more tractable only the zeroth order term in the parenthesis on the right hand side of Eq. (3) will be used for the following calculations. Numerical testing has shown that this assumption makes a negligible difference for the parameter ranges of interest here.

The expression for the outward speed is then given by

$$\frac{dR}{dt} = \sqrt{\frac{4\sigma}{\rho R^2}\frac{2r_1r_2}{(r_1+r_2)}}, \tag{4}$$

which can be integrated to give the neck radius with time,

$$R = 2\left(\frac{2\sigma r_1 r_2}{\rho(r_1+r_2)}\right)^{1/4} t^{1/2}. \tag{5}$$

We will now check this model against the data from Thoroddsen *et al.*[5] Equation (4) has a similar form to the capillary-inertial model described in that paper. That model includes an adjustable constant C, whereas there are no adjustable parameters in the simple model presented here. Their data fit the capillary-inertial model very well if C is given a value of 1.08. Equation (4) in this paper can be used to predict a value of 1.41 for C if $r_1 = r_2$ (to match the model of Thoroddsen *et al.*) and $(z_1+z_2)/r \ll 1$, which is a valid assumption at early times during the growth of the neck. Figure 2(a) shows the data from Fig. 4 of Thoroddsen *et al.* compared with the results from Eq. (5). The dynamical model presented in this paper overpredicts the speed of the neck growth, which is expected because there are no energy loss terms included, and simplifying assumptions were made about the shape of the neck. However, the general form of the function is the same and this model includes the effects of r_1 and r_2. The author is unaware of coalescence speed data for coalescing bubbles where the parent bubble's radius ratio was more than 2, so Eq. (5) remains untested for higher radius ratios. However, the model predicts the correct order of magnitude and the correct functional form, providing confidence that a first-order calculation of the acoustic forcing can be made with this model.

Equation (5) can be used to find the volume gained by the new bubble with time, so the acoustic forcing provided by the dynamics of the coalescence event can now be calculated directly. The additional bubble volume after time t, $\Delta V(t)$ is given by

$$\Delta V(t) = \int_0^{r=R(t)} 2\pi R dR(z_1+z_2). \tag{6}$$

Using small angle assumptions for θ_1 and θ_2 and Eq. (5), this reduces to

$$\Delta V(t) = \frac{8\pi\sigma}{\rho}t^2. \tag{7}$$

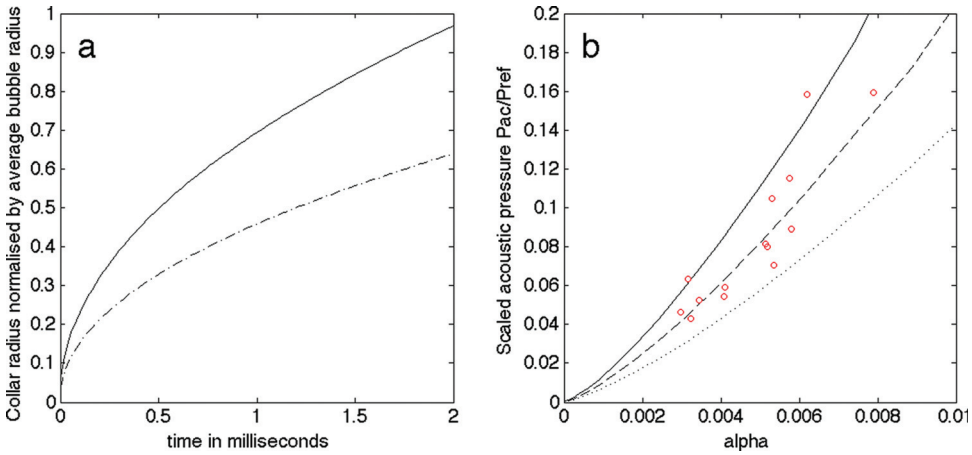

Fig. 2. (Color online) (a) A plot of the neck width with time. The dotted line shows the results from Thoroddsen *et al.* and the solid line shows the predictions of the model described in this paper for the same parameters. If the model results are multiplied by 0.65, they exactly overlie the experimental data. (b) The scaling of the acoustic pressure amplitude with a reference pressure, a plot equivalent to figure 13 in Manasseh *et al.* The circles are the data points from that figure, and the lines show the predictions from the model presented here for θ_{lim} of 40° (dotted line), 45° (dashed line), and 50° (solid line).

The effect of this additional bubble volume will be to decrease the pressure inside the bubble. The change in external pressure that would be required to account for this change in bubble volume can be calculated using the polytropic relationship

$$P_{\text{in}} = P_{\text{in},0}\left(\frac{V_0}{V_0 + \Delta V}\right)^{\kappa}, \tag{8}$$

where P_{in} is the internal bubble pressure at the time of interest, and $P_{\text{in},0}$ is the internal bubble pressure when the bubble is in equilibrium with the ambient pressure in the liquid around it. $\frac{\Delta V}{V_0} \ll 1$, so a binomial expansion of Eq. (8) yields the forcing function $f(t)$ for a spherical bubble of radius R_0,

$$f(t) = \frac{-6\sigma\kappa P_{\text{in},0}}{\rho^2 R_0^5} t^2. \tag{9}$$

The additional factor of ρR_0^2 in Eq. (9) is due to the form in which the forcing is inserted into the Rayleigh–Plesset equation, as an equivalent external pressure.[4] This forcing term can then be used to drive the linearized Rayleigh–Plesset equation, once the appropriate time dependence is taken into account (discussed below). To apply the Rayleigh–Plesset equation, it is necessary to use an equivalent spherical radius for the new bubble, and we assume here that the breathing mode response of the bubble can be described using spherical symmetry. This approach produced good results in Deane and Czerski.[4]

Equation (9) has no dependence on the parent bubble radii. The most obvious effect that the bubble radii will have is to limit the length of time for which this simple model of neck expansion is valid. We make the assumption here that this is controlled by the smaller bubble of the pair (labeled bubble 2), and that the length of time for which forcing continues is related to the length of time taken for the neck radius to reach some fixed fraction of the small bubble radius, or equivalently a limiting angle $\theta_2 = \theta_{\text{lim}}$. The calculation here is carried out with values for θ_{lim} of 40, 45, and 50 degrees, so that the importance of this parameter can be judged. The time taken for the neck to reach this radius [calculated using Eq. (5) and labeled t_{lim}] will be used to scale the time for which the forcing is allowed to continue.

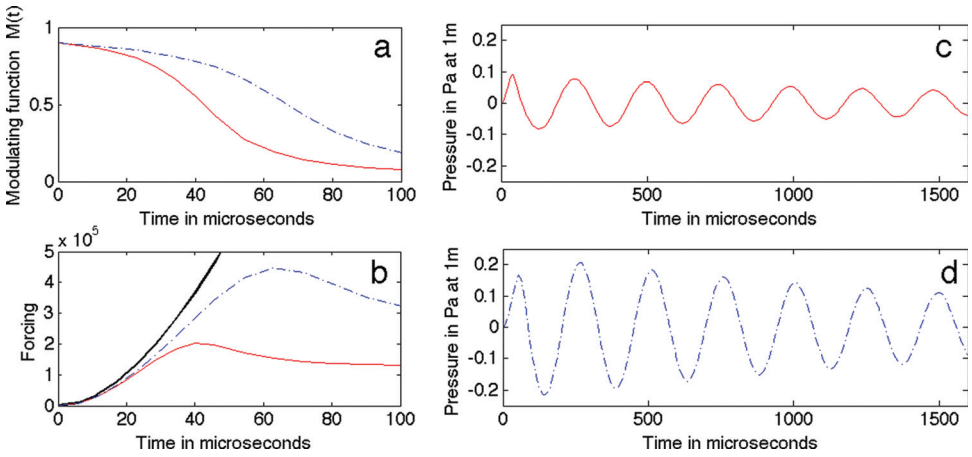

Fig. 3. (Color online) Results of the model described in this paper, from numerical simulations using the parameters in Manasseh's paper. The large bubble has a radius of 0.8 mm in all cases, and the results shown here are for small bubble radii of 150 μm (solid line) and 200 μm (dashed line). (a) The function modulating the forcing for the two radii. In each case, the modulating function $M(t)$ passes through 0.5 at t_{lim}. (b) The forcing functions. The thick solid line shows the unmodulated forcing function $f(t)$, and the thin solid and dashed lines show the final forcing functions for the two bubble radii, once that modulating function is applied. (c) and (d) The calculated acoustic pressures with time for these situations. The vertical axis is the same in both plots, and it can be seen that both pressure signals rise initially, and that the amplitude of the pulse associated with the 200 μm radius bubble is much larger than that associated with the 150 μm radius bubble.

The arbitrary function chosen to modulate the forcing is an arctangent, because this is continuously differentiable and relatively straightforward to scale. The modulating function $M(t)$ is shown below, and its effect on the forcing function is shown in Fig. 3,

$$M(t) = \frac{1}{2} - \frac{1}{\pi}\arctan\left(B\frac{t - t_{\mathrm{lim}}}{t_{\mathrm{lim}}}\right), \tag{10}$$

where B is a constant chosen to determine the cut-off slope. The $M(t)$ scales so that it is close to 1 at time zero and has decreased to 0.5 at t_{lim}. The value for B used in these calculations was chosen to be 3 to provide a reasonable cut-off slope.

With the acoustical model in place, it is now possible to calculate the acoustic pressure signals produced by coalescence events. The outcomes of this model will be compared with the data of Manasseh *et al.*[3] The radii of the new bubbles in that study have a minimum value of 0.8 mm, so we neglect the change in internal pressure due to surface tension. The newly coalesced bubble will oscillate close to its natural frequency, so for the damping term we use Medwin's approximation.[6] The version of the Rayleigh–Plesset equation used here is

$$\frac{d^2\varepsilon}{dt^2} = -\frac{3\kappa P_0}{\rho R_0^2}\varepsilon - 0.0025 f^{\frac{1}{3}}\omega\frac{d\varepsilon}{dt} + \left[\frac{1}{2} - \frac{1}{\pi}\arctan\left(B\frac{t - t_{\mathrm{lim}}}{t_{\mathrm{lim}}}\right)\right]\frac{6\kappa\sigma P_0}{\rho^2 R_0^5}t^2, \tag{11}$$

where ω is the natural frequency of the new bubble in radians/s, f is equal to $\omega/2\pi$, R_0 is the equivalent spherical radius of the new bubble, and ε is the fractional change in bubble radius. Integrating this with respect to time gives us the bubble wall radius, speed, and acceleration; so the acoustic pressure at 1 m distance can be calculated.

In the experiments of Manasseh *et al.* a large bubble was formed at a nozzle, followed by a much smaller bubble that coalesced with the first bubble after a short interval. High-speed photography was used to measure the bubble radii and a nearby hydrophone recorded the acoustic pulse produced. The effects of reverberation in the

tanks were checked and found to be negligible. The first observation to note is that initially the sound pressure in the experiments of Manasseh *et al.* always rose, contrasting with the observations of bubble pinch-off where the sound pressure was always observed to fall initially. This is consistent with the volume oscillations being driven by a rapid change in bubble volume, since in the pinch-off experiments the bubble volume decreases rapidly, whereas during the coalescence process the volume increases rapidly.

The major acoustic result is shown in Fig. 13 of the paper by Manasseh *et al.* where the ratio of bubble volumes is shown to have an approximately linear relationship with the scaled acoustic pressure amplitude. In order to compare the model presented here with those data, equivalent numerical simulations of those experiments have been carried out using the model described above and the results have been plotted in the same way for comparison. Equation (11) was integrated with respect to time for an appropriate range of small bubble radii, and for one large bubble radius (0.8 mm). The acoustic pressure amplitude was extracted from the numerical simulations in the same way that it was extracted from the experimental data.

The comparison is shown in Fig. 2(b). It can be seen that the predicted acoustic amplitudes match the data very well, and that the predicted relationship between alpha and the scaled acoustic pressure is consistent with the data. It should be remembered that Eq. (5) overestimated the collapse speed, so the model is also expected to overestimate the acoustical pressure amplitude and this is not the case here. However, considering the many first-order assumptions in the model outlined in this paper, the agreement in pressure amplitude is acceptable.

3. Conclusions

A simple dynamical model for the growth of a neck of air between two coalescing bubbles has been shown to produce the correct functional form and approximately the right order of magnitude, providing confidence that it could be used for first-order calculations of the rate of volume change with time. The length of time for which the volume forcing continued was controlled by a simple modulating relationship that depended on the size of the smaller bubble of the pair. This acoustic forcing was then used to drive the linearized Rayleigh–Plesset equations to calculate the acoustic pressure pulses expected from coalescing bubbles driven by this mechanism. A comparison of the results with published data shows that the mechanism of volume forcing generates the right order of magnitude for the acoustical amplitude. In addition, it can also account for the observed relationship between the size of the smaller bubble and the amplitude of the emitted sound, and the sign of the initial change in pressure is correctly predicted. Rapid volume change due to the bubble dynamics has previously been shown to be a significant mechanism for driving the sound produced by fragmenting bubbles, and the calculations here suggest that it is also a mechanism driving sound emission during bubble coalescence.

Acknowledgments

The author wishes to thank Grant Deane for his helpful discussions, and Richard Manasseh for providing the experimental data shown in Fig. 2(b). This work was supported by the Natural Environment Research Council (Grant No. NE/H016856/1).

References and links

[1]M. Strasberg, "Gas bubbles as sources of sound in liquids," J. Acoust. Soc. Am. **28**, 20–26 (1956).
[2]T. G. Leighton, K. J. Fagan, and J. E. Field, "Acoustic and photographic studies of injected bubbles," Eur. J. Phys. **12**, 77–85 (1991).
[3]R. Manasseh, G. Riboux, and F. Risso, "Sound generation on bubble coalescence following detachment," Int. J. Multiphase Flow **34**, 938–949 (2008).
[4]G. B. Deane and H. Czerski, "A mechanism stimulating sound production from air bubbles released from a nozzle," J. Acoust. Soc. Am. **123**, EL126–EL132 (2008).
[5]S. T. Thoroddsen, T. G. Etoh, K. Takehara, and N. Ootsuka, "On the coalescence speed of bubbles," Phys. Fluids **17**, 071703 (2005).
[6]H. Medwin, *Sounds in the Sea* (Cambridge University Press, Cambridge, 2005), Eq. 6.72b, p. 187.